Rem: Revista Escola de Minas
ISSN: 0370-4467
editor@rem.com.br
Escola de Minas
Brasil

Moraes Barreto Campello, Eduardo; Mattos Pimenta, Paulo de; Wriggers, Peter
Elastic-plastic analysis of metallic shells at finite strains
Rem: Revista Escola de Minas, vol. 60, núm. 2, abril-junio, 2007, pp. 381-389
Escola de Minas
Ouro Preto, Brasil

Elastic-plastic analysis of metallic shells at finite strains

(Análise elasto-plástica de cascas metálicas por deformações finitas)

Eduardo Moraes Barreto Campello
Polytechnic School at the University of São Paulo, P.O. Box 61548, São Paulo, 05424-970, Brazil
E-mail: campello@usp.br

Paulo de Mattos Pimenta
Polytechnic School at the University of São Paulo, P.O. Box 61548, São Paulo, 05424-970, Brazil
E-mail: ppimenta@usp.br

Peter Wriggers
Institute of Mechanics and Computational Mechanics, University of Hanover, Appelstrasse 9A, Hanover, 30167, Germany. E-mail: wriggers@ibnm.uni-hannover.de

Resumo

Nesse trabalho, a teoria de cascas geometricamente exata, que considera a variação da espessura apresentada em [1], é estendida para o caso de materiais metálicos. Elasticidade finita isótropa, nas deformações logarítmicas, e o critério de plastificação de von Mises são adotados. A teoria é implementada, computacionalmente, com a ajuda do elemento finito triangular T6-3i de [1], cujo desempenho é avaliado por meio de dois exemplos numéricos.

Palavras-chave: Elastoplasticidade, cascas elastoplásticas, deformações finitas, rotações finitas, variação da espessura, elemento finito triangular de casca.

Abstract

The geometrically-exact finite-strain variable-thickness shell model of [1] is reviewed in this paper and extended to the case of metallic elastoplastic shells. Isotropic elasticity and von Mises yield criterion with isotropic hardening are considered. The model is implemented within a triangular finite element and is briefly assessed by means of two numerical examples.

Keywords*: Elastoplasticity, Elastic-plastic shells, finite strains, finite rotations, variable-thickness, triangular shell finite element.*

1. Introduction

The main purpose of this work is to extend the geometrically-exact finite-strain variable-thickness shell formulation of [1] to the case of metallic elastoplastic shells. The shell motion is described by a director theory with a standard Reissner-Mindlin kinematical assumption, and the Euler-Rodrigues formula is utilized in order to represent finite rotations in a fully exact manner.

Our approach to elastoplasticity combines the multiplicative decomposition of the deformation gradient with the concept of an instantaneous natural configuration. The elastic domain is defined on the principal axes of the right Cauchy-Green elastic strain tensor, through a logarithmic neo-Hookean material law. A von Mises yield function with isotropic hardening is adopted for constraining the admissible states, and as a result, the classical radial return method (see e.g. [2,3]) may be straightforwardly employed for integration of the stresses.

The model is implemented over the six-node triangular finite element of [1] and is briefly assessed by means of two numerical examples.

2. Shell theory

A flat reference configuration is assumed for the shell mid-surface at the outset. A unit orthogonal system $\{\boldsymbol{e}_1^r, \boldsymbol{e}_2^r, \boldsymbol{e}_3^r\}$ is defined (see Figure 1) so that points in this configuration are described by the vector field

$$\boldsymbol{\xi} = \boldsymbol{\zeta} + \zeta \boldsymbol{e}_3^r \tag{1}$$

where $\boldsymbol{\zeta} = \xi_\alpha \boldsymbol{e}_\alpha^r$ describes the position of points at the middle surface and $\zeta \boldsymbol{e}_3^r$ is the shell reference director. $\zeta \in H\,[-h^b,\ h^t]$ is the thickness coordinate.

Let now $\{\boldsymbol{e}_1, \boldsymbol{e}_2, \boldsymbol{e}_3\}$ be a local orthogonal system on the current configuration, with $\boldsymbol{e}_i = \boldsymbol{Q}\boldsymbol{e}_i^r$ as depicted in Figure 1. Here $\boldsymbol{Q} = \hat{\boldsymbol{Q}}(\boldsymbol{\theta})$ is the rotation tensor and $\boldsymbol{\theta}$ the rotation vector. On this configuration the position of the shell material points is given by

$$\boldsymbol{x} = \boldsymbol{z} + s\boldsymbol{e}_3 \tag{2}$$

where $\boldsymbol{z} = \hat{\boldsymbol{z}}(\xi_\alpha)$ represents the position of points at the middle surface and

$$s = (1+p)\zeta + \frac{1}{2}q\zeta^2 \tag{3}$$

describes the position of points along the current director $\boldsymbol{e}_3$. Note that a quadratic distribution for s was assumed. This is the simplest assumption that avoids the so-called Poisson's locking. The scalar parameters $p = \hat{p}(\xi_\alpha)$ and $q = \hat{q}(\xi_\alpha)$ are transversal degrees-of-freedom that depicts the constant and the linear parts of the strains related to the thickness change.

The rotation tensor $\boldsymbol{Q}$ may be expressed by the well-known Euler-Rodrigues formula

$$\boldsymbol{Q} = \boldsymbol{I} + h_1(\boldsymbol{\theta})\boldsymbol{\Theta} + h_2(\boldsymbol{\theta})\boldsymbol{\Theta}^2 \tag{4}$$

in which $\theta = \|\boldsymbol{\theta}\|$ is the true rotation angle and $\boldsymbol{\Theta} = \mathrm{Skew}(\boldsymbol{\theta})$ is the skew-symmetric tensor whose axial vector is $\boldsymbol{\theta}$. Here, the following trigonometric functions are introduced for use along the text

$$h_1(\theta) = \frac{\sin\theta}{\theta}, \quad h_2(\theta) = \frac{1}{2}\frac{\sin^2(\theta/2)}{(\theta/2)^2}, \quad h_3(\theta) = \frac{1-h_1(\theta)}{\theta^2}$$
$$h_4(\theta) = \frac{h_1(\theta)-2h_2(\theta)}{\theta^2} \quad \text{and} \quad h_5(\theta) = \frac{h_2(\theta)-3h_3(\theta)}{\theta^2}. \tag{5}$$

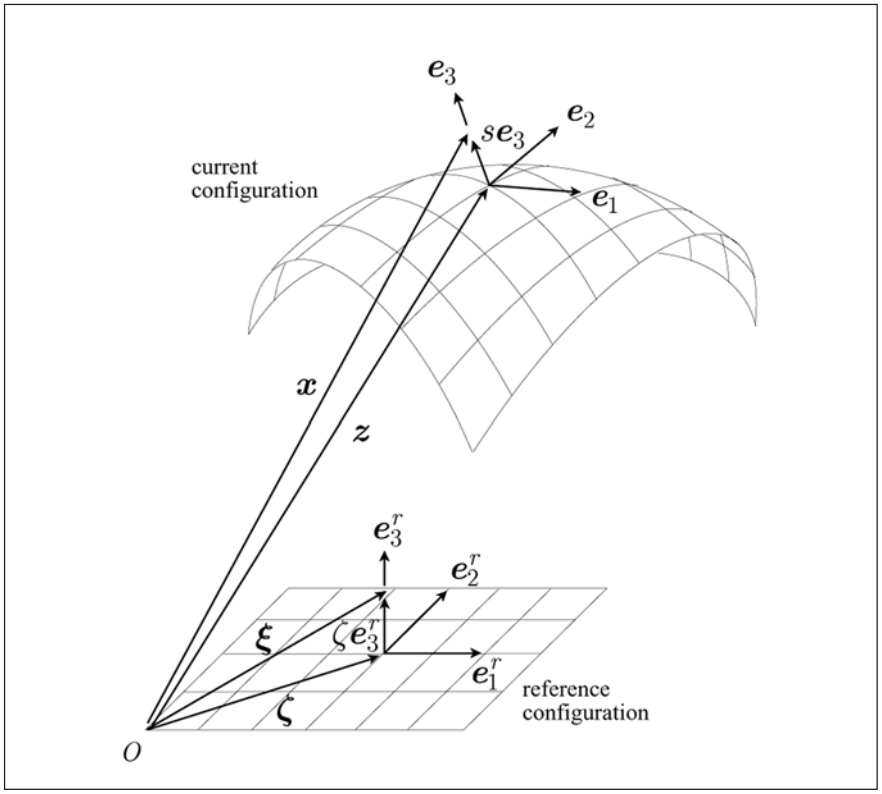

Figure 1 - Shell description and basic kinematical quantities.

The displacement vector for points on the reference mid-surface is $\boldsymbol{u} = z - \zeta$. Components of $\boldsymbol{u}$ and $\boldsymbol{\theta}$ together with scalars p and q define the 8 degrees-of-freedom of this shell theory:

$$\boldsymbol{d} = [\, \boldsymbol{u} \;\; \boldsymbol{\theta} \;\; p \;\; q \,]^T \tag{6}$$

The deformation gradient $\boldsymbol{F}$ is evaluated from differentiation of (2) with respect to $\boldsymbol{\xi}$, and after some algebra one has

$$\boldsymbol{F} = \boldsymbol{Q}[\boldsymbol{I} + \boldsymbol{\gamma}_\alpha^r \otimes \boldsymbol{e}_\alpha^r + \boldsymbol{\gamma}_3^r \otimes \boldsymbol{e}_3^r] = \boldsymbol{Q}\boldsymbol{F}^r \tag{7}$$

where

$$\begin{aligned} &\boldsymbol{\gamma}_\alpha^r = \boldsymbol{\eta}_\alpha^r + s_{,\alpha}\boldsymbol{e}_3^r + s\boldsymbol{\kappa}_\alpha^r \times \boldsymbol{e}_3^r, \quad \boldsymbol{\gamma}_3^r = s'\boldsymbol{e}_3^r, \\ &\boldsymbol{\eta}_\alpha^r = \boldsymbol{Q}^T\boldsymbol{z}_{,\alpha} - \boldsymbol{e}_\alpha^r \quad \text{and} \quad \boldsymbol{\kappa}_\alpha^r = \boldsymbol{\Gamma}^T\boldsymbol{\theta}_{,\alpha}, \end{aligned} \tag{8}$$

with the notation $(\bullet)_{,\alpha} = \partial(\bullet)/\partial\xi_\alpha$ and $(\bullet)' = \partial(\bullet)/\partial\zeta$ for derivatives. Tensor $\boldsymbol{\Gamma}$ in $(8)_4$ is

$$\boldsymbol{\Gamma} = \boldsymbol{I} + h_2(\boldsymbol{\theta})\boldsymbol{\Theta} + h_3(\boldsymbol{\theta})\boldsymbol{\Theta}^2 \tag{9}$$

Linearization of (7) with respect to $\boldsymbol{d}$ yields the virtual deformation gradient:

$$\delta\boldsymbol{F} = \delta\boldsymbol{\Omega}\boldsymbol{F} + \boldsymbol{Q}[\delta\boldsymbol{\gamma}_i^r \otimes \boldsymbol{e}_i^r] \tag{10}$$

where $d\boldsymbol{W} = \delta\boldsymbol{Q}\boldsymbol{Q}^T$ is a skew-symmetric tensor representing the director virtual spin. Virtual strains $\delta\boldsymbol{\gamma}_i^r$ of (10) are obtained directly from $(8)_{1\text{-}2}$, rendering

$$\delta\boldsymbol{\gamma}_\alpha^r = \delta\boldsymbol{\eta}_\alpha^r + s(\delta\boldsymbol{\kappa}_\alpha^r \times \boldsymbol{e}_3^r) + (\boldsymbol{\kappa}_\alpha^r \times \boldsymbol{e}_3^r)\delta s + \boldsymbol{e}_3^r\delta s_{,\alpha} \quad \text{and} \quad \delta\boldsymbol{\gamma}_3^r = \boldsymbol{e}_3^r\delta s' \tag{11}$$

where

$$\delta\boldsymbol{\eta}_\alpha^r = \boldsymbol{Q}^T\left(\delta\boldsymbol{u}_{,\alpha} + \boldsymbol{Z}_{,\alpha}\boldsymbol{\Gamma}\,\delta\boldsymbol{\theta}\right) \quad \text{and} \quad \delta\boldsymbol{\kappa}_\alpha^r = \boldsymbol{Q}^T\left(\boldsymbol{\Gamma}_{,\alpha}\delta\boldsymbol{\theta} + \boldsymbol{\Gamma}\,\delta\boldsymbol{\theta}_{,\alpha}\right) \tag{12}$$

Here, $\boldsymbol{Z}_{,\alpha} = \text{Skew}(z_{,\alpha})$ and

$$\boldsymbol{\Gamma}_{,\alpha} = h_2(\theta)\boldsymbol{\Theta}_{,\alpha} + h_3(\theta)(\boldsymbol{\Theta}\boldsymbol{\Theta}_{,\alpha} + \boldsymbol{\Theta}_{,\alpha}\boldsymbol{\Theta}) + h_4(\theta)(\boldsymbol{\theta}.\boldsymbol{\theta}_{,\alpha})\boldsymbol{\Theta} + h_5(\theta)(\boldsymbol{\theta}.\boldsymbol{\theta}_{,\alpha})\boldsymbol{\Theta}^2 \tag{13}$$

with $\boldsymbol{\Theta}_{,\alpha} = \text{Skew}(\theta_{,\alpha})$.

Let now the first Piola-Kirchhoff stress tensor be expressed by $\boldsymbol{P} = \boldsymbol{Q}\,\boldsymbol{P}^r$, where $\boldsymbol{P}^r = \boldsymbol{\tau}_i^r \otimes \boldsymbol{e}_i^r$ is its back-rotated counterpart. Vectors $\boldsymbol{\tau}_i^r$ are the back-rotated stress vectors acting on a cross-section normal to $\boldsymbol{e}_i$. With the aid of (10), it is not difficult to show that the shell internal virtual work may be written as

$$\delta W_{\text{int}} = \int_\Omega \int_H (\boldsymbol{P} : \delta\boldsymbol{F})\, d\zeta\, d\Omega = \int_\Omega (\boldsymbol{\sigma} \cdot \delta\boldsymbol{\varepsilon})\, d\Omega \tag{14}$$

in which $\Omega \subset \Re^2$ is the shell domain on the reference middle plane and

$$\begin{aligned} &\boldsymbol{\sigma} = \left[\boldsymbol{n}_1^r \quad \boldsymbol{m}_1^r \quad \boldsymbol{n}_2^r \quad \boldsymbol{m}_2^r \quad P \quad B_1 \quad B_2 \quad Q \quad S_1 \quad S_2\right]^T \quad \text{and} \\ &\boldsymbol{\varepsilon} = \left[\boldsymbol{\eta}_1^r \quad \boldsymbol{\kappa}_1^r \quad \boldsymbol{\eta}_2^r \quad \boldsymbol{\kappa}_2^r \quad p \quad p_{,1} \quad p_{,2} \quad q \quad q_{,1} \quad q_{,2}\right]^T \end{aligned} \tag{15}$$

are 18x1-vectors grouping the cross-sectional resultants and the corresponding strains. In this case,

$$\begin{aligned} &\boldsymbol{n}_\alpha^r = \int_H \boldsymbol{\tau}_\alpha^r d\zeta, \quad \boldsymbol{m}_\alpha^r = \int_H s(\boldsymbol{e}_3^r \times \boldsymbol{\tau}_\alpha^r)\, d\zeta, \\ &P = \int_H [\zeta(\boldsymbol{e}_3^r \times \boldsymbol{\tau}_\alpha^r) \cdot \boldsymbol{\kappa}_\alpha^r + \tau_{33}]\, d\zeta, \quad B_\alpha = \int_H \zeta(\boldsymbol{\tau}_\alpha^r \cdot \boldsymbol{e}_3^r)\, d\zeta, \\ &Q = \int_H \left[\frac{1}{2}\zeta^2(\boldsymbol{e}_3^r \times \boldsymbol{\tau}_\alpha^r) \cdot \boldsymbol{\kappa}_\alpha^r + \zeta\tau_{33}\right] d\zeta \quad \text{and} \quad S_\alpha = \int_H \frac{1}{2}\zeta^2(\boldsymbol{\tau}_\alpha^r \cdot \boldsymbol{e}_3^r)\, d\zeta, \end{aligned} \tag{16}$$

where $\tau_{33} = \boldsymbol{\tau}_3^r \cdot \boldsymbol{e}_3^r$..

The external virtual work may be expressed by

$$\delta W_{\text{ext}} = \int_{\Omega}\left[\overline{\boldsymbol{t}}^{t}\cdot\delta\boldsymbol{x}^{t} + \overline{\boldsymbol{t}}^{b}\cdot\delta\boldsymbol{x}^{b} + \int_{H}\overline{\boldsymbol{b}}\cdot\delta\boldsymbol{x}d\zeta\right]d\Omega = \int_{\Omega}(\overline{\boldsymbol{q}}\cdot\delta\boldsymbol{d})\,d\Omega\,, \tag{17}$$

in which $\overline{\boldsymbol{t}}$ and $\overline{\boldsymbol{b}}$ are the surface and body loadings respectively. Vector $\overline{\boldsymbol{q}}$ groups the generalized external forces, and is given by

$$\overline{\boldsymbol{q}} = \begin{bmatrix}\overline{\boldsymbol{n}} & \boldsymbol{\Gamma}^{T}\overline{\boldsymbol{m}} & \overline{P} & \overline{Q}\end{bmatrix}^{T} \tag{18}$$

where

$$\begin{aligned}
&\overline{\boldsymbol{n}} = \overline{\boldsymbol{t}}^{t} + \overline{\boldsymbol{t}}^{b} + \int_{H}\overline{\boldsymbol{b}}d\zeta\,, \quad \overline{\boldsymbol{m}} = s^{t}\left(\boldsymbol{e}_3\times\overline{\boldsymbol{t}}^{t}\right) + s^{b}\left(\boldsymbol{e}_3\times\overline{\boldsymbol{t}}^{b}\right) + \int_{H}s\left(\boldsymbol{e}_3\times\overline{\boldsymbol{b}}\right)d\zeta\,,\\
&\overline{P} = h^{t}\boldsymbol{e}_3\cdot\overline{\boldsymbol{t}}^{t} - h^{b}\boldsymbol{e}_3\cdot\overline{\boldsymbol{t}}^{b} + \int_{H}\zeta\left(\boldsymbol{e}_3\cdot\overline{\boldsymbol{b}}\right)d\zeta \quad \text{and}\\
&\overline{Q} = \frac{1}{2}\left(h^{t}\right)^{2}\left(\boldsymbol{e}_3\cdot\overline{\boldsymbol{t}}^{t}\right) + \frac{1}{2}\left(h^{b}\right)^{2}\left(\boldsymbol{e}_3\cdot\overline{\boldsymbol{t}}^{b}\right) + \int_{H}\frac{1}{2}\zeta^{2}\left(\boldsymbol{e}_3\cdot\overline{\boldsymbol{b}}\right)d\zeta\,.
\end{aligned} \tag{19}$$

From the virtual work theorem one arrives at the following local equilibrium equations

$$\begin{aligned}
&\boldsymbol{n}_{\alpha,\alpha} + \overline{\boldsymbol{n}} = \boldsymbol{o}\,, \quad \boldsymbol{m}_{\alpha,\alpha} + \boldsymbol{z}_{,\alpha}\times\boldsymbol{n}_{\alpha} + \overline{\boldsymbol{m}} = \boldsymbol{o}\,,\\
&B_{\alpha,\alpha} - P + \overline{P} = 0 \quad \text{and} \quad S_{\alpha,\alpha} - Q + \overline{Q} = 0\,,
\end{aligned} \tag{20}$$

where $\boldsymbol{n}_{\alpha} = \boldsymbol{Q}\boldsymbol{n}_{\alpha}^{r}$ and $\boldsymbol{m}_{\alpha} = \boldsymbol{Q}\boldsymbol{m}_{\alpha}^{r}$ are the sectional forces at the current configuration. The Fréchet derivative of $\delta W = \delta W_{\text{int}} - \delta W_{\text{ext}}$ with respect to $\boldsymbol{d}$ leads to the tangent bilinear form

$$\delta^{*}(\delta W) = \int_{\Omega}\left[(\boldsymbol{\Psi}\delta\boldsymbol{d})\cdot\left(\boldsymbol{D}\boldsymbol{\Psi}\,\delta^{*}\boldsymbol{d}\right) + (\boldsymbol{\Delta}\delta\boldsymbol{d})\cdot(\boldsymbol{G}\boldsymbol{\Delta}\delta^{*}\boldsymbol{d}) - \delta\boldsymbol{d}\cdot\boldsymbol{L}\delta^{*}\boldsymbol{d}\right]d\Omega\,, \tag{21}$$

where

$$\begin{aligned}
&\boldsymbol{\Psi} = \begin{bmatrix}\overline{\boldsymbol{\Psi}} & \boldsymbol{o} & \boldsymbol{o}\\ \boldsymbol{O} & \boldsymbol{\psi} & \boldsymbol{o}\\ \boldsymbol{O} & \boldsymbol{o} & \boldsymbol{\psi}\end{bmatrix}, \quad \boldsymbol{D} = \frac{\partial\boldsymbol{\sigma}}{\partial\boldsymbol{\varepsilon}}, \quad \boldsymbol{\Delta} = \begin{bmatrix}\boldsymbol{\Delta}_1 & \boldsymbol{o} & \boldsymbol{o}\\ \boldsymbol{\Delta}_2 & \boldsymbol{o} & \boldsymbol{o}\end{bmatrix}, \quad \boldsymbol{G} = \begin{bmatrix}\boldsymbol{G}_1 & \boldsymbol{O}\\ \boldsymbol{O} & \boldsymbol{G}_2\end{bmatrix},\\
&\boldsymbol{L} = \frac{\partial\overline{\boldsymbol{q}}}{\partial\boldsymbol{d}}, \quad \overline{\boldsymbol{\Psi}} = \begin{bmatrix}\boldsymbol{\Psi}_1\\ \boldsymbol{\Psi}_2\end{bmatrix}, \quad \boldsymbol{\Psi}_{\alpha} = \begin{bmatrix}\boldsymbol{Q}^{T} & \boldsymbol{O}\\ \boldsymbol{O} & \boldsymbol{Q}^{T}\end{bmatrix}\begin{bmatrix}\boldsymbol{I} & \boldsymbol{O} & \boldsymbol{Z}_{,\alpha}\boldsymbol{\Gamma}\\ \boldsymbol{O} & \boldsymbol{\Gamma} & \boldsymbol{\Gamma}_{,\alpha}\end{bmatrix}\boldsymbol{\Delta}_{\alpha},\\
&\boldsymbol{\psi} = \begin{bmatrix}1 & \dfrac{\partial}{\partial\xi_1} & \dfrac{\partial}{\partial\xi_2}\end{bmatrix}^{T} \quad \text{and} \quad \boldsymbol{\Delta}_{\alpha} = \begin{bmatrix}\boldsymbol{I}\dfrac{\partial}{\partial\xi_{\alpha}} & \boldsymbol{O} & \boldsymbol{O}\\ \boldsymbol{O} & \boldsymbol{I}\dfrac{\partial}{\partial\xi_{\alpha}} & \boldsymbol{I}\end{bmatrix}^{T}.
\end{aligned} \tag{22}$$

Submatrices $\boldsymbol{G}_{\alpha}$ of $\boldsymbol{G}$ can be found in [1], while submatrices of $\boldsymbol{D}$ are computed by the chain rule with the aid of the following quantities

$$\frac{\partial\boldsymbol{\tau}_{\alpha}^{r}}{\partial\boldsymbol{\gamma}_{\beta}^{r}} = \boldsymbol{C}_{\alpha\beta}^{r}\,, \quad \boldsymbol{c}_{\alpha}^{r} = \frac{\partial\boldsymbol{\tau}_{\alpha}^{r}}{\partial\gamma_{33}} = \frac{\partial\tau_{33}}{\partial\boldsymbol{\gamma}_{\alpha}^{r}} \quad \text{and} \quad c^{r} = \frac{\partial\tau_{33}}{\partial\gamma_{33}} \tag{23}$$

where $\gamma_{33} = \boldsymbol{\gamma}_{3}^{r}\cdot\boldsymbol{e}_{3}^{r} = s'$ (again, see [1] for the detailed expressions).

3. Tangent Moduli

Let $\boldsymbol{S}$ be the second Piola-Kirchhoff stress tensor and $\boldsymbol{E}$ the Green-Lagrange strain tensor. The fourth-order tensor of tangent moduli associated with the pair $\{\boldsymbol{S}, \boldsymbol{E}\}$ is defined by

$$\mathbb{D} = \frac{\partial \boldsymbol{S}}{\partial \boldsymbol{E}} \tag{24}$$

The back-rotated first Piola-Kirchhoff stress tensor $\boldsymbol{P}^r = \boldsymbol{Q}^T\boldsymbol{P} = \boldsymbol{\tau}_i^r \otimes \boldsymbol{e}_i^r$ is related to $\boldsymbol{S}$ through $\boldsymbol{P}^r = \boldsymbol{F}^r\boldsymbol{S}$. If one introduces the following third- and second-order tangent tensors

$$\boldsymbol{\mathcal{B}}_\alpha = \frac{\partial \boldsymbol{E}}{\partial \boldsymbol{\gamma}_\alpha^r} \quad \text{and} \quad \boldsymbol{B} = \frac{\partial \boldsymbol{E}}{\partial \gamma_{33}}, \tag{25}$$

then it is possible to write

$$\begin{aligned} &\boldsymbol{\tau}_\alpha^r = \boldsymbol{\mathcal{B}}_\alpha^T \boldsymbol{S}, \quad \tau_{33} = \boldsymbol{B} : \boldsymbol{S}, \quad \boldsymbol{C}_{\alpha\beta}^r = \boldsymbol{\mathcal{B}}_\alpha^T \mathbb{D} \boldsymbol{\mathcal{B}}_\beta + (\boldsymbol{e}_\alpha^r \cdot \boldsymbol{S}\boldsymbol{e}_\beta^r)\boldsymbol{I}, \\ &\boldsymbol{c}_\alpha^r = \boldsymbol{\mathcal{B}}_\alpha^T \mathbb{D}\boldsymbol{B} + (\boldsymbol{e}_\alpha^r \cdot \boldsymbol{S}\boldsymbol{e}_3^r)\boldsymbol{e}_3^r \quad \text{and} \quad c^r = \boldsymbol{B} : \mathbb{D}\boldsymbol{B} + \boldsymbol{e}_3^r \cdot \boldsymbol{S}\boldsymbol{e}_3^r . \end{aligned} \tag{26}$$

Expressions $(26)_{1\text{-}2}$ can be used in (16), while $(26)_{3\text{-}5}$ can be used in (23) for the computation of $\boldsymbol{D}$.

4. Constitutive equation

4.1 Logarithmic neo-Hookean material

Let λ_i (i = 1,2,3) be the principal values of $\boldsymbol{U} = (\boldsymbol{F}^T\boldsymbol{F})^{1/2}$ and $\boldsymbol{V} = (\boldsymbol{F}\boldsymbol{F}^T)^{1/2}$. Let $\boldsymbol{v}_i$ (i = 1, 2, 3) be a principal triad of $\boldsymbol{V}$. Let $\varepsilon_i = \ln \lambda_i$ be the principal logarithmic strains, and let us define the following strain invariants: $\vartheta = \ln J = \varepsilon_1 + \varepsilon_2 + \varepsilon_3$, where $J = \lambda_1\lambda_2\lambda_3$, and $\overline{I} = (1/2)\left(\overline{\varepsilon}_1^2 + \overline{\varepsilon}_2^2 + \overline{\varepsilon}_3^2\right)$, with $\overline{\varepsilon}_i = \varepsilon_i - (1/3)\vartheta$ (notice that $\overline{\varepsilon}_i = \ln \overline{\lambda}_i$, with $\overline{\lambda}_i = J^{-1/3}\lambda_i$).). A neo-Hookean isotropic elastic material can be defined by the specific strain energy function below

$$\psi\left(\vartheta, \overline{I}\right) = \kappa \frac{1}{2}\vartheta^2 + 2\mu\overline{I}, \tag{27}$$

where κ and μ are material parameters. From this expression, the Kirchhoff-Trefftz stress tensor reads

$$\boldsymbol{\Sigma} = \sum_{i=1}^{3}\left(\Sigma_i \boldsymbol{v}_i \otimes \boldsymbol{v}_i\right), \quad \text{where} \quad \Sigma_i = \kappa\vartheta + \overline{\Sigma}_i, \quad \text{with} \quad \overline{\Sigma}_i = 2\mu \ln \overline{\lambda}_i, \tag{28}$$

in which Σ_i are the principal values of $\boldsymbol{\Sigma}$. The second Piola-Kirchhoff stress tensor is then given by

$$\boldsymbol{S} = \mathbb{F}^{-T}\boldsymbol{\Sigma} = \boldsymbol{F}^{-1}\boldsymbol{\Sigma}\boldsymbol{F}^{-T}, \tag{29}$$

where $\mathbb{F}$ is a fourth-order tensor that performs a congruent transformation on $\boldsymbol{\Sigma}$. The related tensor of tangent moduli $\mathbb{D}$, as first derived in [2] (see also [4,5]), can be written as follows

$$\mathbb{D} = \mathbb{F}^{-T}(\mathbb{E} + \mathbb{G} - \mathbb{S})\mathbb{F}^{-1}, \tag{30}$$

where

$$\begin{aligned} &\mathbb{E} = \kappa \boldsymbol{I} \otimes \boldsymbol{I} + 2\mu\mathbb{M}, \quad \mathbb{M} = \mathbb{I} - \frac{1}{3}\boldsymbol{I} \otimes \boldsymbol{I}, \\ &\mathbb{G} = \sum_{i,j=1, i\neq j}^{3}\left(G_{ij} + G_{ji} - 2\mu\right)\left(\boldsymbol{v}_i \otimes \boldsymbol{v}_j \otimes \boldsymbol{v}_i \otimes \boldsymbol{v}_j\right), \\ &G_{ij} = \left(\frac{\lambda_i^2}{\lambda_j^2} - 1\right)^{-1}\left(\Sigma_i - \Sigma_j\right) \quad \text{and} \\ &\mathbb{S} = \sum_{i,j=1}^{3}\left(\Sigma_i + \Sigma_j\right)\left(\boldsymbol{v}_i \otimes \boldsymbol{v}_j \otimes \boldsymbol{v}_i \otimes \boldsymbol{v}_j\right). \end{aligned} \tag{31}$$

4.2 Von Mises plasticity

Our basic kinematical assumption in describing an elastoplastic deformation is the multiplicative decomposition of the deformation gradient, in the form $\boldsymbol{F} = \boldsymbol{F}^{\mathrm{e}}\,\boldsymbol{F}^{\mathrm{p}}$. Here $\boldsymbol{F}^{\mathrm{e}}$ represents the elastic part of the deformation and $\boldsymbol{F}^{\mathrm{p}}$ the natural configuration. We assume that $\boldsymbol{F}^{\mathrm{p}} = \boldsymbol{F}^{\mathrm{p}}(t)$ (t = time) describes the plastic deformation, with $\boldsymbol{F}^{\mathrm{p}}(0)$ being the initial natural configuration set as $\boldsymbol{F}^{\mathrm{p}}(0) = \boldsymbol{I}$.

The elastic and the plastic deformation gradients have the polar decompositions $\boldsymbol{F}^{\mathrm{e}} = \boldsymbol{R}^{\mathrm{e}}\boldsymbol{U}^{\mathrm{e}} = \boldsymbol{V}^{\mathrm{e}}\boldsymbol{R}^{\mathrm{e}}$ and $\boldsymbol{F}^{\mathrm{p}} = \boldsymbol{R}^{\mathrm{p}}\boldsymbol{U}^{\mathrm{p}}$, where $\boldsymbol{U}^{\mathrm{e}} = (\boldsymbol{F}^{\mathrm{eT}}\boldsymbol{F}^{\mathrm{e}})^{1/2}$ is the right elastic stretching tensor, $\boldsymbol{V}^{\mathrm{e}} = \boldsymbol{R}^{\mathrm{e}}\boldsymbol{U}^{\mathrm{e}}\boldsymbol{R}^{\mathrm{eT}} = (\boldsymbol{F}^{\mathrm{e}}\boldsymbol{F}^{\mathrm{eT}})^{1/2}$ is the left elastic stretching tensor, $\boldsymbol{R}^{\mathrm{e}}$ is the elastic rotation tensor, $\boldsymbol{U}^{\mathrm{p}}$ is the right plastic stretching tensor and $\boldsymbol{R}^{\mathrm{p}}$ is the plastic rotation tensor.

We relate the Kirchhoff-Trefftz stress tensor to the elastic part of the deformation through the isotropic neo-Hookean law of (27). A von Mises yield function with isotropic hardening constrains the elastic domain as below

$$F(\boldsymbol{S}^{\mathrm{e}}) = \bar{\sigma} - \sigma_{\mathrm{y}}(\alpha) \leq 0\,, \quad \text{where} \quad \bar{\sigma} = \sqrt{\frac{3}{2}\bar{\boldsymbol{S}}^{\mathrm{e}} : \bar{\boldsymbol{S}}^{\mathrm{e}}} = \sqrt{\frac{3}{2}\bar{\boldsymbol{\Sigma}} : \bar{\boldsymbol{\Sigma}}} \tag{32}$$

In this case, $\boldsymbol{S}^{\mathrm{e}} = \boldsymbol{R}^{\mathrm{eT}}\boldsymbol{\Sigma}\boldsymbol{R}^{\mathrm{e}}$ is the Green-Naghdi stress tensor and $\bar{\boldsymbol{S}}^{\mathrm{e}} = \mathbb{M}\boldsymbol{S}^{\mathrm{e}}$ is its deviatoric part, while $\bar{\boldsymbol{\Sigma}} = \mathbb{M}\boldsymbol{\Sigma}$ is the deviatoric part of $\boldsymbol{\Sigma}$. Still in (32), α is the equivalent plastic strain. From the normality law we have

$$\dot{\boldsymbol{E}}^{\mathrm{p}} = \mathrm{Sym}\left(\dot{\boldsymbol{U}}^{\mathrm{p}}\boldsymbol{U}^{\mathrm{p}-1}\right) = \dot{\alpha}\boldsymbol{N}\,, \quad \dot{\alpha} \geq 0\,, \quad \boldsymbol{N} = \frac{\partial F}{\partial \boldsymbol{S}^{\mathrm{e}}} = \frac{3}{2\bar{\sigma}}\bar{\boldsymbol{S}}^{\mathrm{e}} \tag{33}$$

where the superposed dot denotes time differentiation.

Let us consider now the material state at instant t_i, at which $\boldsymbol{F}_i$, $\boldsymbol{U}_i^{\mathrm{p}}$ and α_i are supposed to be known. One thus has

$$\boldsymbol{F}_i^{\mathrm{e}} = \boldsymbol{F}_i\boldsymbol{U}_i^{\mathrm{p}-1} \tag{34}$$

Performing the polar decomposition $\boldsymbol{F}_i^{\mathrm{e}} = \boldsymbol{R}_i^{\mathrm{e}}\boldsymbol{U}_i^{\mathrm{e}}$, the stress tensor at this instant may be computed by $\boldsymbol{S}_i^{\mathrm{e}} = \mathbb{E}^{\mathrm{e}}\boldsymbol{E}_i^{\mathrm{e}}$, where $\boldsymbol{E}_i^{\mathrm{e}} = \ln\boldsymbol{U}_i^{\mathrm{e}}$ and $\mathbb{E}^{\mathrm{e}} = \kappa\boldsymbol{I}\otimes\boldsymbol{I} + 2\mu\mathbb{M}$. At instant t_{i+1} only the deformation gradient $\boldsymbol{F}_{i+1}$ is assumed to be known, and the following trial elastic state is defined assuming that the plastic part of the deformation has not changed

$$\boldsymbol{F}_t^{\mathrm{e}} = \boldsymbol{F}_{i+1}\boldsymbol{U}_i^{\mathrm{p}-1} \tag{35}$$

With $\boldsymbol{F}_t^{\mathrm{e}} = \boldsymbol{R}_t^{\mathrm{e}}\boldsymbol{U}_t^{\mathrm{e}}$, the stress tensor in this state is obtained via $\boldsymbol{S}_t^{\mathrm{e}} = \mathbb{E}\boldsymbol{E}_t^{\mathrm{e}}$, where $\boldsymbol{E}_t^{\mathrm{e}} = \ln\boldsymbol{U}_t^{\mathrm{e}}$. If $F_t = F(\boldsymbol{S}_t) < 0$, then the trial state is an admissible one, i.e. $\Delta\alpha$ and

$$\boldsymbol{S}_{i+1}^{\mathrm{e}} = \boldsymbol{S}_t^{\mathrm{e}}\,, \quad \alpha_{i+1} = \alpha_i \quad \text{and} \quad \boldsymbol{U}_{i+1}^{\mathrm{p}} = \boldsymbol{U}_i^{\mathrm{p}} \tag{36}$$

However, if $F_t \geq 0$, there is an incremental plastic stretching $\Delta\boldsymbol{U}^{\mathrm{p}}$ such that

$$\boldsymbol{F}_{i+1}^{\mathrm{e}} = \boldsymbol{F}_t^{\mathrm{e}}\,, \quad \Delta\boldsymbol{U}^{\mathrm{p}-1}\boldsymbol{F}_{i+1}^{\mathrm{p}} = \Delta\boldsymbol{U}^{\mathrm{p}}\boldsymbol{U}_i^{\mathrm{p}} \quad \text{and} \quad \boldsymbol{U}_{i+1}^{\mathrm{p}} = \left(\boldsymbol{F}_{i+1}^{\mathrm{p}\,T}\boldsymbol{F}_{i+1}^{\mathrm{p}}\right)^{1/2} \tag{37}$$

The incremental stress integration algorithm is then formulated by the following constrained minimization problem, which must be solved for $\boldsymbol{S}_{i+1}^{\mathrm{e}}$:

$$\min\left[\frac{1}{2}(\boldsymbol{S}_{i+1}^{\mathrm{e}} - \boldsymbol{S}_t^{\mathrm{e}}) : \mathbb{E}^{-1}(\boldsymbol{S}_{i+1}^{\mathrm{e}} - \boldsymbol{S}_t^{\mathrm{e}})\right] \quad \text{subjected to} \quad F(\boldsymbol{S}_{i+1}^{\mathrm{e}}, \alpha_{i+1}) = 0 \tag{38}$$

For the von Mises yield function (32) the analytical solution of (38) is given by

$$\boldsymbol{S}_{i+1}^{\mathrm{e}} = \boldsymbol{S}_t^{\mathrm{e}} + \frac{\sigma_{\mathrm{y}}(\alpha_{i+1}) - \bar{\sigma}_t}{\bar{\sigma}_t}\bar{\boldsymbol{S}}_t^{\mathrm{e}}\,, \quad \text{where} \quad \sigma_{\mathrm{y}}(\alpha_{i+1}) = \sigma_{\mathrm{y}}(\alpha_i + \Delta\alpha) \tag{39}$$

which is the well-known radial return method. Hence, $\Delta\alpha$ is the solution of the equation

$$3\mu\Delta\alpha + \sigma_{\mathrm{y}}(\alpha_i + \Delta\alpha) - \bar{\sigma}_t = 0 \tag{40}$$

(in the case of linear hardening an explicit solution is attained). The radial return algorithm is summarized below:

1) Trial step:

$$\boldsymbol{F}_t^{\mathrm{e}} = \boldsymbol{F}_{i+1}\boldsymbol{U}_i^{\mathrm{p}-1}\ ; \quad \boldsymbol{U}_t^{\mathrm{e}} = \left(\boldsymbol{F}_t^{\mathrm{e}T}\boldsymbol{F}_t^{\mathrm{e}}\right)^{1/2}\ ; \quad \boldsymbol{R}_t^{\mathrm{e}} = \boldsymbol{F}_t^{\mathrm{e}}\boldsymbol{U}_t^{\mathrm{e}-1}\ ; \quad \boldsymbol{E}_t^{\mathrm{e}} = \ln \boldsymbol{U}_t^{\mathrm{e}}\ ;$$

$$\boldsymbol{S}_t^{\mathrm{e}} = \mathbb{E}^{\mathrm{e}}\boldsymbol{E}_t^{\mathrm{e}}\ ; \quad \boldsymbol{\Sigma}_t = \boldsymbol{R}_t^{\mathrm{e}}\boldsymbol{S}_t^{\mathrm{e}}\boldsymbol{R}_t^{\mathrm{e}T}\ ; \quad \bar{\sigma}_t = \sqrt{\frac{3}{2}\bar{\boldsymbol{\Sigma}}_t : \bar{\boldsymbol{\Sigma}}_t}\ ; \quad F_t = \bar{\sigma}_t - \sigma_{\mathrm{y}}(\alpha_i)\ ;$$

2) Radial return algorithm:

if $(F_t < 0)$ then !(elastic step)

$$\alpha_{i+1} = \alpha_i\ ; \quad \boldsymbol{U}_{i+1}^{\mathrm{p}} = \boldsymbol{U}_i^{\mathrm{p}}\ ; \quad \boldsymbol{\Sigma}_{i+1} = \boldsymbol{\Sigma}_t\ ; \quad \mathbb{E} = \mathbb{E}^{\mathrm{e}}\ ;$$

else if $(F_t \geq 0)$ then !(elastic-plastic step)

Solve $\quad 3\mu\Delta\alpha + \sigma_{\mathrm{y}}(\alpha_i + \Delta\alpha) - \bar{\sigma}_t = 0 \quad$ for $\ \Delta\alpha\ ; \quad \alpha_{i+1} = \alpha_i + \Delta\alpha\ ;$

$$\Delta\boldsymbol{E}^{\mathrm{p}} = \frac{3\Delta\alpha}{2\bar{\sigma}_t}\bar{\boldsymbol{S}}_t^{\mathrm{e}}\ ; \quad \Delta\boldsymbol{U}^{\mathrm{p}} = e^{\Delta\boldsymbol{E}^{\mathrm{p}}}\ ; \quad \boldsymbol{F}_{i+1}^{\mathrm{p}} = \Delta\boldsymbol{U}^{\mathrm{p}}\,\boldsymbol{U}_i^{\mathrm{p}}\ ;$$

$$\boldsymbol{U}_{i+1}^{\mathrm{p}} = \left(\boldsymbol{F}_{i+1}^{\mathrm{p}T}\boldsymbol{F}_{i+1}^{\mathrm{p}}\right)^{1/2}\ ; \quad \boldsymbol{\Sigma}_{i+1} = \boldsymbol{\Sigma}_t - \frac{3\mu\Delta\alpha}{\bar{\sigma}_t}\bar{\boldsymbol{\Sigma}}_t\ ;$$

$$\mathbb{E} = \mathbb{E}^{\mathrm{e}} - 2\mu\frac{3\mu\Delta\alpha}{\bar{\sigma}_t}\mathbb{M} - \frac{3\mu}{\bar{\sigma}_t^2}\left(\frac{3\mu\Delta\alpha}{\bar{\sigma}_t} + \frac{3\mu}{3\mu + h_{i+1}}\right)\bar{\boldsymbol{\Sigma}}_t \otimes \bar{\boldsymbol{\Sigma}}_t\ ;$$

end if .

5. Numerical examples

The present model is implemented over the six-node flat triangular element introduced by the authors in [1]. The displacements $\boldsymbol{u}$ are approximated with quadratic functions, while a linear interpolation scheme is adopted for the rotation vector $\boldsymbol{\theta}$ and for the thickness parameters p and q. No special techniques such as ANS, EAS or reduced-integration with hourglass control are necessary and the element is a pure displacement-based one. Either shear or membrane locking are not observed.

5.1 Bending of square plate

A quadratic plate under constant dead load is considered here similarly to [6,7]. The vertical displacements at the edges of the plate are restricted to zero, and symmetry conditions are adopted. Problem data and analysis results are shown in Figure 2.

5.2 Pinched hemisphere

A relatively thick hemispherical shell (see [8,9]) is loaded by two pairs of collinear forces, as in Figure 3. Symmetry conditions are used so that only one quadrant of the structure needs to be modeled. Geometry and material data are also shown in Figure 3, together with the results obtained.

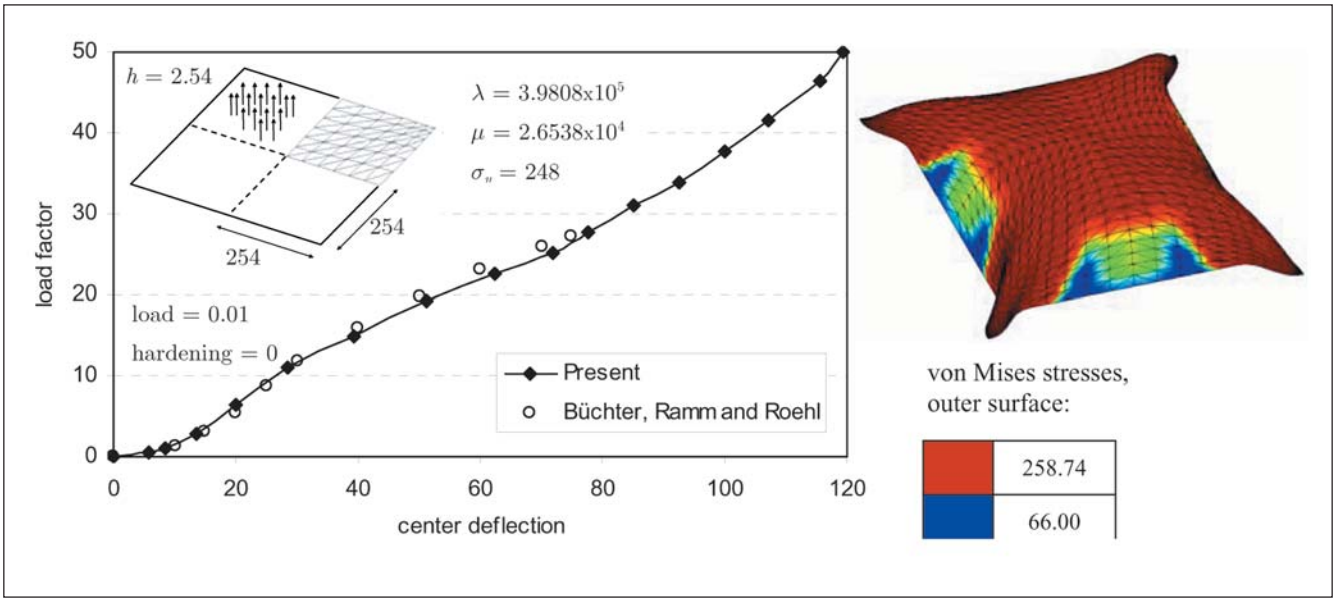

Figure 2 - Problem data and analysis results for Example 5.1.

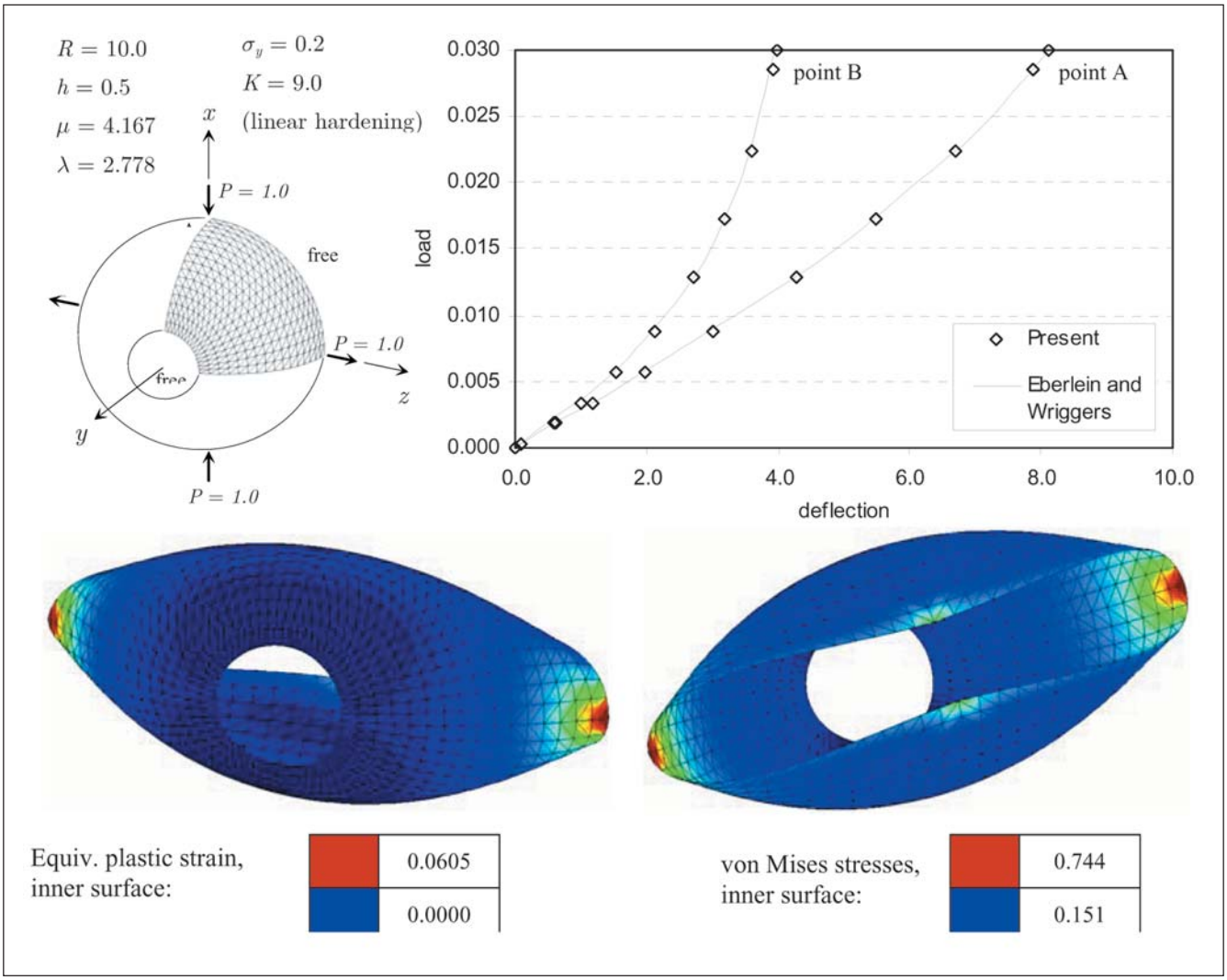

Figure 3 - Problem data and analysis results for Example 5.2.

6. Conclusions

The geometrically-exact finite-strain shell model of [1] was extended here to the case of elastic-plastic shells. Good performance of the formulation can be observed via numerical assessment. We believe that simple but reliable triangular elements combined with stable hardening-plasticity models are an excellent tool for the nonlinear elastoplastic analysis of shell structures.

7. Acknowledgements

Fellowship funding from FAPESP (*Fundação de Amparo à Pesquisa do Estado de São Paulo*), CNPq (*Conselho Nacional de Pesquisa*) and DFG (*Deutsche Forschungsgemeinschat*), as well as the material support from IBNM (*Institut für Baumechanik und Numerische Mechanik*) are gratefully acknowledged by the first two authors in this work.

8. References

[1] PIMENTA, P.M., CAMPELLO, E. M. B. , WRIGGERS, P. A fully nonlinear multi-parameter shell model with thickness variation and a triangular shell finite element. ***Comput. Mech.***, 34, p.181-193, 2004.

[2] PIMENTA, P. M. Finite-deformation soil plasticity on principal axes, Proceedings of the 3rd COMPLAS, CIMNE, Barcelona, 1992.

[3] SIMO, J. C., HUGHES, T. J. R. ***Computational Inelasticity***, Springer-Verlag, New York, 1998.

[4] PIMENTA, P. M. A stress integration algorithm for the analysis of elastic-plastic solids by the finite element method. I. Small strain analysis. Technical Report BT/PEF-8913, Department of Structural and Foundation Engineering, Polytechnic School at the University of São Paulo, 1989.

[5] PIMENTA, P. M. A stress integration algorithm for the analysis of elastic-plastic solids by the finite element method. II. Large deformation analysis. Technical Report BT/PEF-8914, Department of Structural and Foundation Engineering, Polytechnic School at the University of São Paulo, 1989.

[6] BÜCHTER, N., RAMM, E. E., ROEHL, D. "3-D extension of nonlinear shell formulation based on the EAS concept. ***Int. J. Numer. Meth. Engrg.***, 37, p. 2551-2568, 1994.

[7] RAMM, E. E., MATZENMILLER, A. Consistent linearization in elastoplastic shell analysis. ***Eng. Comp.***, 5, p.289-299, 1988.

[8] EBERLEIN, R., WRIGGERS, P. FE concepts for finite elastoplastic strains and isotropic stress response in shells: theoretical and computational analysis. ***Comput. Meth. Appl. Mech. Engrg.***, 171, p. 243-279, 1999.

[9] SIMO, J. C., KENNEDY, J. G. On a stress resultant geometrically exact shell model. Part V. Nonlinear plasticity: formulation and integration algorithms. ***Comp. Meth. Appl. Mech. Engrg.***, 96, p. 133-171, 1992.

Artigo recebido em 27/11/2006 e aprovado em 29/01/2007.